ACS APPLIED MATERIALS & INTERFACES

Research Article

www.acsami.org

Chemically Functionalized Conjugated Oligoelectrolyte Nanoparticles for Enhancement of Current Generation in Microbial Fuel Cells

Cui-e Zhao,[†] Jia Chen,[†,‡] Yuanzhao Ding,[§] Victor Bochuan Wang,[†,§] Biqing Bao,[‡] Staffan Kjelleberg,[§,∥] Bin Cao,[§,⊥] Say Chye Joachim Loo,[†,§] Lianhui Wang,*[,‡] Wei Huang,*[,‡,#] and Qichun Zhang*[,†,▽]

[†]School of Materials Science and Engineering, Nanyang Technological University, Singapore 639798, Singapore

[‡]Key Laboratory for Organic Electronics & Information Displays (KLOEID) and Institute of Advanced Materials (IAM), Nanjing University of Posts & Telecommunications, Nanjing 210023, China

[§]Singapore Centre on Environmental Life Sciences Engineering, Nanyang Technological University, Singapore 637551, Singapore

[∥]School of Biotechnology and Biomolecular Sciences and Centre for Marine Bio-innovation, The University of New South Wales, Sydney New South Wales 2052, Australia

[⊥]School of Civil and Environmental Engineering, Nanyang Technological University, Singapore 637551, Singapore

[#]Jiangsu−Singapore Joint Research Center for Organic/Bio-Electronics & Information Displays and Institute of Advanced Materials, Nanjing Tech University, Nanjing, China

[▽]Division of Chemistry and Biological Chemistry, School of Physical and Mathematical Sciences, Nanyang Technological University, Singapore 637371, Singapore

Supporting Information

ABSTRACT: Water-soluble conjugated oligoelectrolyte nanoparticles (COE NPs), consisting of a cage-like polyhedral oligomeric silsesquioxanes (POSS) core equipped at each end with pendant groups (oligo(*p*-phenylenevinylene) electrolyte, OPVE), have been designed and demonstrated as an efficient strategy in increasing the current generation in *Escherichia coli* microbial fuel cells (MFCs). The as-prepared COE NPs take advantage of the structure of POSS and the optical properties of the pendant groups, OPVE. Confocal laser scanning microscopy showed strong photoluminescence of the stained cells, indicating spontaneous accumulation of COE NPs within cell membranes. Moreover, the electrochemical performance of the COE NPs is superior to that of an established membrane intercommunicating COE, DSSN+ in increasing current generation, suggesting that these COE NPs thus hold great potential to boost the performance of MFCs.

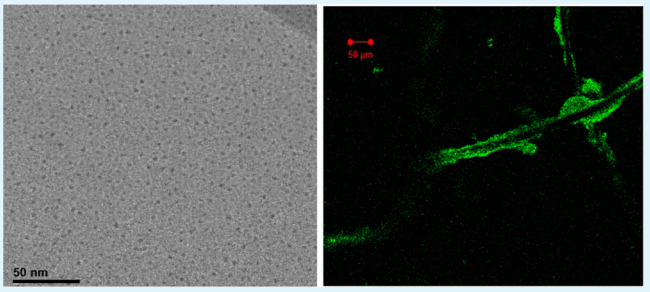

KEYWORDS: *conjugated oligoelectrolyte (COE), nanoparticles, polyhedral oligomeric silsesquioxanes (POSS), current generation, microbial fuel cells*

1. INTRODUCTION

Microbial fuel cells (MFCs) have received extensive attention as an alternative renewable power source in recent years.[1,2] In MFCs, electrochemically active bacteria decompose an organic substrate into small molecules and transfer the electrons produced during the metabolic process to the electrode at the anaerobic anode.[3−5] The transfer of electrons from the internal metabolic cycles may occur by a variety of extracellular electron transfer pathways, including outer membrane *c*-type cytochromes, conductive nanowires, and electron shuttle molecules.[6,7] The electrons then move farther across an external load to the cathode and reduce the electron acceptors, resulting in the generation of electrical power simultaneously from organic waste. However, the relatively low power density of MFCs, due to poor extracellular electron transfer (EET) between bacteria cells and the electrode, still limits their practical applications.[8−10]

The performance of MFCs is highly dependent on the microbial metabolism, electrode material and reactor design.[11−16] Recently, extensive studies have been devoted to accelerate electron transfer in MFCs. One possible solution is to develop efficient anode materials to enhance the interaction between the electrode and bacteria, as the EET between anode and biofilm directly determines the bioelectrochemical

Received: May 8, 2015
Accepted: June 16, 2015
Published: June 16, 2015

ACS Publications © 2015 American Chemical Society

DOI: 10.1021/acsami.5b03990
ACS Appl. Mater. Interfaces 2015, 7, 14501−14505

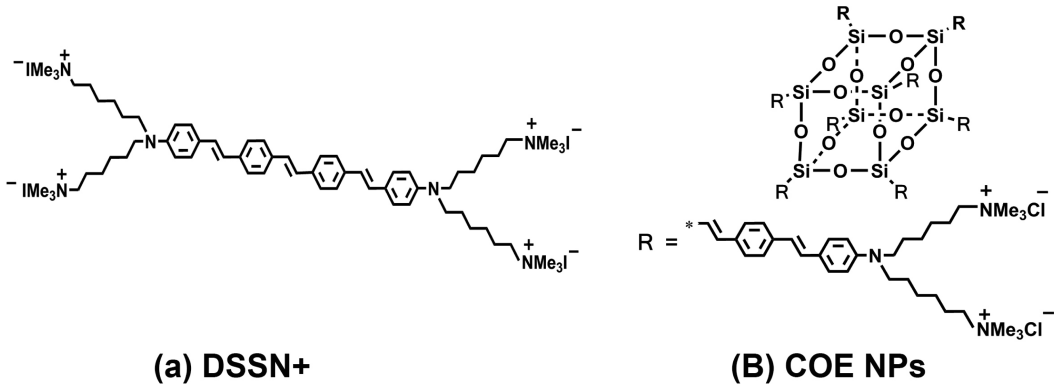

Figure 1. Chemical structures of (a) DSSN+ and (b) COE NPs.

processes.[17−21] Another possible solution is to facilitate EET from the interior of the bacterial cell out to the electrode. For example, biogenic inorganic nanoparticles have been exploited to coat the cell membrane of Shewanella PV-4 to enhance EET.[22] In a different approach, Bazan and co-workers[23] have shown that microorganisms can be modified by the insertion of conjugated oligoelectrolytes (COEs) into the microbial membrane to improve charge transport across lipid bilayers in MFCs.

COEs are a class of synthetic molecules containing an electronically π-delocalized backbones appended with ionic functionalities.[24] Several types of COEs have been demonstrated to be effective in facilitating EET across the microbial membrane. One special example of this is (4,4′-bis(4′-(*N*,*N*-bis(6″-(*N*,*N*,*N*-trimethylammonium)hexyl)-amino)-styryl)-stilbene tetraiodide) (DSSN+),[25] a linear oligo-phenylenevinylene with pendant ionic groups at the two terminal ends of its long axis (Figure 1a). On the other hand, polyhedral oligomeric silsesquioxanes (POSS) are cage-like nanostructured materials (typically $R_8Si_8O_{12}$) that consist of a nanometer-sized siloxane cube (diameter ca. 0.5 nm).[26] The introduction of POSS into the organic network could remarkably enhance the mechanical and optical properties due to their organic−inorganic hybrid structure.[27] Moreover, the rigid and bulky POSS have already been employed as building blocks for the construction of luminescent molecules and polymers to improve solubility and their quantum yields.[28] If π-conjugated repeat units [i.e. oligo(p-phenylenevinylene) electrolyte (OPVE)] were used as arms to attach on each corner of the cubic POSS, water-soluble COE NPs could be synthesized (Figure 1b). In addition, we believe that COE NPs might provide more redox centers, which could help enhance the current generation.

Here, we report the successful preparation of water-soluble COE NPs, and investigate that the addition of these NPs leads to an increase of current generation in *Escherichia coli*-based MFCs, as compared to the control MFC without COE modification. Confocal laser scanning microscopy (CLSM) showed strong photoluminescence (PL) of the stained cells, indicating spontaneous accumulation of COE NPs within cell membranes. The electrochemical performance of COE NPs is comparable to that of an established membrane intercommunicating COE (i.e. DSSN+). These findings point toward the potential of COE NPs in facilitating EET in MFCs.

2. EXPERIMENTAL SECTION

2.1. Chemicals and Equipment. (1-Bromo-4-(bromomethyl) benzene and trimethylamine (ethanol solution) were purchased from Sigma-Aldrich. Aniline was purchased from Alfa Aesar. DSSN+ was synthesized according to previously reported procedures.[29] All materials were used as received unless otherwise stated. Solution NMR spectra were taken on a Bruker Advance 400 spectrometer. High-resolution transmission electron microscope (HR-TEM) images were obtained using a JEOL JEM-2100 at an accelerating voltage of 200 kV. UV−vis absorption spectra were recorded on a UV-3600 Shimadzu UV−vis Spectrophotometer. Fluorescence emission spectra were obtained using Shimadzu RF 5301 PC. The PL quantum yield was performed on an Edinburgh FL 920 instrument.

2.2. Bacterial Strain. *E. coli* K-12 (ATCC #10798) was purchased from American Type Culture Collection (Manassas, VA). *E. coli* K-12 was cultured aerobically in a 50 mL tube containing sterile Luria−Bertani (LB) broth medium at 37 °C overnight on a shaker (150 rpm). LB medium was prepared from trypticase peptone (10 g L^{-1}), yeast extract (5 g L^{-1}), and sodium chloride (10 g L^{-1}) dissolved in ultrapure water and sterilized by autoclaving. Ultrapure water was obtained from a Millipores Milli-Q water purification system (Billerica, MA). All media and solutions were sterilized before use.

2.3. MFC Construction and Data Acquisition. Dual-chamber MFCs were constructed from two glass bottles joined by a glass tube. After sterilization and removal of the ultrapure water, the anode chamber was filled with sterile LB medium and 1 mL of live cell culture solution, while the catholyte was 50 mM $K_3Fe(CN)_6$ solution with 100 mM phosphate buffer solution (PBS). Carbon felt (3.18 mm thickness, VWR Pte. Ltd., Singapore, 8 cm^2) were used as the electrodes. The anode and the cathode were separated from each other by a piece of proton exchange membrane (Nafion N117 0.18 mm, Sigma-Aldrich, Singapore). The electrodes were then connected to a 1000 Ω resistor with titanium wire and voltage measurements across the resistor were recorded at a rate of 1 point per 5 min using eDAQ e-corders data acquisition system (Colorado Springs, CO) equipped with Chart software. The power density curves were collected by switching resistors (50−100 000 Ω). Power was calculated using $P = IV$. The MFCs were operated at 30 °C, and all devices were sterilized before use. All runs were conducted three times.

2.4. Confocal Laser Scanning Microscopy. Carbon felt electrodes were removed from operating MFCs and *E. coli* stained with DSSN+, and COE NPs colonized on carbon felt electrodes were for imaging purposes. Confocal laser scanning microscopy (CLSM, Carl Zeiss Microscopy LSM 780) was used to acquire confocal fluorescence images, and the resulting images were analyzed using IMARIS software (version 7.6.4; Bitplane, Zurich, Switzerland).

2.5. Scanning Electron Microscopy (SEM). SEM images were collected using a JEOL/JSM-6340F FE-SEM at an acceleration voltage of 5 kV. At the end of the MFC runs, the carbon felt anodes were removed from the MFCs and fixed in 2.5% glutaraldehyde for 1 h, dehydrated in a series of ethanol solutions (25, 50, 75, 95, and 100%), and then vacuum-dried. Samples were coated with Au prior to SEM imaging.

DOI: 10.1021/acsami.5b03990
ACS Appl. Mater. Interfaces 2015, 7, 14501−14505

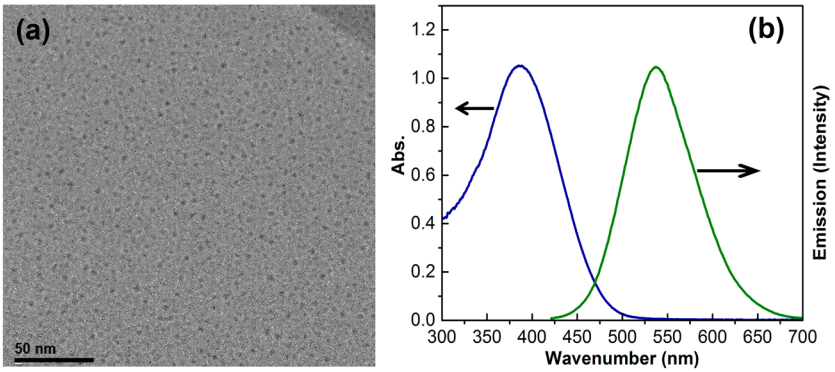

Figure 2. (a) HR-TEM image and (b) UV−vis spectrum and PL profile of the COE NPs (50 μM) in 2 mM PBS solution.

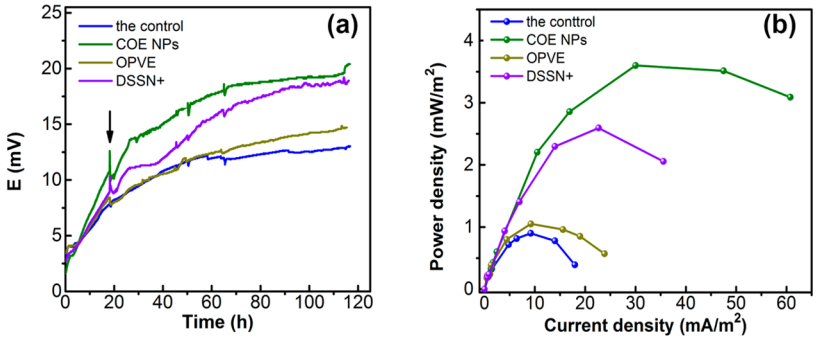

Figure 3. (a) Voltage generation and (b) power curves of *E. coli* MFCs with the control, COE NPs, OPVE, and DSSN+. The arrow indicates the addition of COE NPs, OPVE, and DSSN+.

3. RESULTS AND DISCUSSION

3.1. Preparation and Characterization of COE NPs. The synthesis of water-soluble COE NPs is shown in Scheme S1 (Supporting Information), in which the OPVE was attached onto the eight corners of POSS through Heck coupling reaction. The morphology of the as-prepared water-soluble COE NPs (uniform size ~4.7 nm) was evaluated by high-resolution transmission electron microscopy (HR-TEM; Figure 2a). The UV−vis absorption spectrum and PL feature of the obtained COE NPs in water were also characterized. As shown in Figure 2b, a broad absorption peak centered at about 390 nm was observed, which could be assigned to the pendant units.[30] The fluorescent emission of the COE NPs was located at 550 nm with a quantum yield (φf) of 12%.[31] More importantly, the COE NPs could maintain 80% of its PL intensity under ultrastrong UV light, while the PL intensity of the single branched chain (OPVE) decreased dramatically under UV light (Figure S3, Supporting Information), indicating that attaching COEs to POSS could greatly enhance their optical stability in water. This is because employing rigid and bulky POSS core as the scaffold could remarkably improve the stability of COE NPs due to their organic−inorganic hybrid structure and spherical shape.

3.2. Performance of COE NPs in MFCs. To investigate the performance of the COE NPs in MFCs, *E. coli* was chosen as the model microbe because it is readily available, easily cultured, nonpathogenic, and not strongly electrogenic. A classic dual-chamber MFC with ferricyanide solution in the cathode chambers was constructed. One batch of cell culture was used to inoculate all MFCs with the same number of *E. coli* cells, COE NPs, OPVE, and DSSN+ (both 5 μM) were added to the MFC anode chambers, respectively. The control MFC did not contain any COE NPs or DSSN+. The voltage generations of MFCs were obtained (Figure 3a). It was observed that *E. coli* MFCs with both COE NPs and DSSN+ produced higher voltage than the OPVE MFC and the control MFC. Specifically, the MFC modified with the COE NPs produced a steady state power generation up to 20 mV and the MFC modified with DSSN+ produced 18 mV, whereas the OPVE MFC and the control MFC produced 13 and 12 mV, respectively. The voltage measurements for each MFC were conducted with good reproductivity between each of the data sets. The as-prepared COE NPs could enhance the electrical performance of MFCs through enhanced EET, which was attributed to the spherical structures with multiple functionalized arms.

To better examine the performance of COE NPs modified MFCs, we measured power generation curves by varying the external resistance. Notably, the power outputs of the COE NPs and DSSN+ modified MFCs were greatly improved as compared to the OPVE MFC and the control MFC (Figure 3b). The maximum power density of the MFCs modified with COE NPs showed a 4-fold improvement over the control (3.6 vs 0.9 mW/m^2), while the OPVE and DSSN+ MFC showed a 1.2-fold and 2.5-fold improvement (1.1 vs 0.9 mW/m^2, and 2.5 vs 0.9 mW/m^2), respectively. These results reveal that the COE NPs play a significant role in the power generation of MFCs. It is worth noting that the power density of the COE-NP-modified MFC is comparable to previously reported COE-incorporated *E. coli* MFCs, but the molecular structures are different.[32] It has been proposed that linear COEs function as molecular wires that incorporate into cell membranes to facilitate EET in MFCs.[29] Another possible mechanism to explain the enhanced power output is through the release of

DOI: 10.1021/acsami.5b03990
ACS Appl. Mater. Interfaces 2015, 7, 14501−14505

cytosolic components due to cell membranes perturbation during COE incorporation.[33]

CLSM images of the anode electrodes after MFC operation were collected. Because no additional fluorophore was added to the system, no emission was observed from the control anode from the unmodified MFCs (Figure 4a). In the case of cells

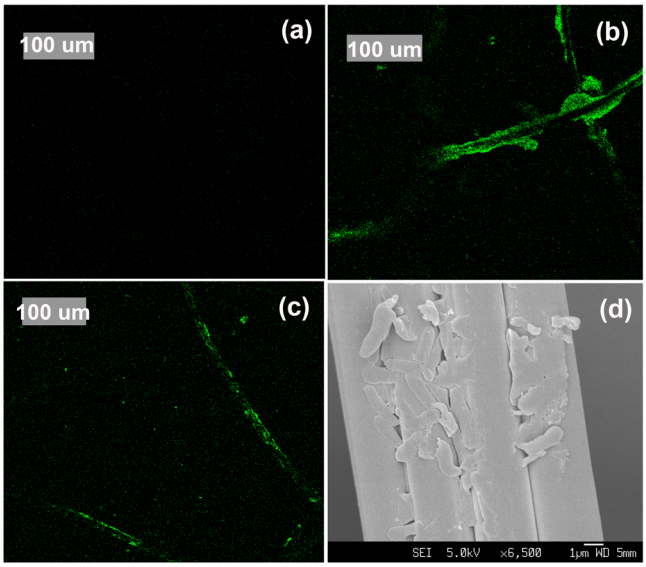

Figure 4. CLSM images of *E. coli* (a) without staining and (b and c) stained with COE NPs and DSSN+. (d) SEM image of *E.coli* adhered to carbon felt surface.

stained with COEs, it is evident that COE NPs and DSSN+ accumulated within membranes (Figures 4b,c), respectively, to exhibit fluorescence. Such studies were aided by COEs exhibiting intrinsic fluorescence via excitation by a 488 nm laser source. To confirm the attachment of *E. coli* to the electrode surface, we employed scanning electron microscopy (SEM) to characterize the surface. Accumulation of cells was observed on the electrode surface (Figure 4d).

4. CONCLUSION

In summary, new water-soluble COE NPs have been designed and synthesized. The as-prepared NPs take advantage of the structure of POSS and the optical properties of the pendant groups OPVEs. The COE NPs successfully incorporate into cell membranes to enhance EET in COE-NP-modified *E. coli* MFCs. Of practical significance is the superiority of the COE NPs over the widely studied DSSN+ in increasing current generation. These COE NPs thus hold great potential to boost the performance of MFCs, suggesting that new COE structures may be discovered to better improve interactions at the bacteria-electrode interface.

■ ASSOCIATED CONTENT

Supporting Information

Preparation and characterization of the COE NPs. The Supporting Information is available free of charge on the ACS Publications website at DOI: 10.1021/acsami.5b03990.

■ AUTHOR INFORMATION

Corresponding Authors

* E-mail: qczhang@ntu.edu.sg.
* E-mail: iamlhwang@njupt.edu.cn.
* E-mail: iamwhuang@njtech.edu.cn.

Notes

The authors declare no competing financial interest.

■ ACKNOWLEDGMENTS

Q.Z. acknowledges financial support from Academic Research Fund Tier 1 (RG 133/14) and Tier 2 (ARC 20/12 and ARC 2/13) from the Ministry of Education, Singapore, the CREATE program (Nanomaterials for Energy and Water Management) from the National Research Foundation, and the New Initiative Fund from NTU, Singapore. S.C.J.L. would like to acknowledge financial support from the Singapore Centre on Environmental Life Sciences Engineering (SCELSE) (M4330001.C70.703012), School of Materials Science and Engineering (M020070110), and the NTU-National Healthcare Group (NTU-NHG) grant (ARG/14012). L.H.W. acknowledges financial support from the Ministry of Education of China (IRT1148) and the Priority Academic Program Development of Jiangsu Higher Education Institutions (PAPD).

■ REFERENCES

(1) Logan, B. E. Exoelectrogenic Bacteria That Power Microbial Fuel Cells. *Nat. Rev. Microbiol.* **2009**, *7*, 375−381.
(2) Zhao, C.-E.; Wu, J.; Kjelleberg, S.; Loo, J. S. C.; Zhang, Q. Employing Flexible and Low-Cost Polypyrrole Nanotube Membrane As an Anode to Enhance Current Generation in Microbial Fuel Cells. *Small* **2015**, DOI: 10.1002/smll.201403328.
(3) Yang, Y.; Xiang, Y.; Sun, G.; Wu, W.-M.; Xu, M. Electron Acceptor-Dependent Respiratory and Physiological Stratifications in Biofilms. *Environ. Sci. Technol.* **2015**, *49*, 196−202.
(4) Gao, Y.; An, J.; Ryu, H.; Lee, H. S. Microbial Fuel Cells as Discontinuous Portable Power Sources: Syntropic Interactions with Anode-Respiring Bacteria. *ChemSusChem* **2014**, *7*, 1026−1029.
(5) Xiao, L.; He, Z. Applications and Perspectives of Phototrophic Microorganisms for Electricity Generation from Organic Compounds in Microbial Fuel Cells. *Renew. Sus. Energy Rev.* **2014**, *37*, 550−559.
(6) Malvankar, N. S.; Lovley, D. R. Microbial Nanowires for Bioenergy Applications. *Curr. Biotechnol.* **2014**, *27*, 88−95.
(7) Fitzgerald, L. A.; Petersen, E. R.; Ray, R. I.; Little, B. J.; Cooper, C. J.; Howard, E. C.; Ringeisen, B. R.; Biffinger, J. C. *Shewanella oneidensis* MR-1 Msh pilin proteins are involved in extracellular electron transfer in microbial fuel cells. *Process Biochem.* **2012**, *47*, 170−174.
(8) Yong, Y.-C.; Dong, X.-C.; Chan-Park, M. B.; Song, H.; Chen, P. Macroporous and Monolithic Anode Based on Polyaniline Hybridized Three-Dimensional Graphene for High-Performance Microbial Fuel Cells. *ACS Nano* **2012**, *6*, 2394−2400.
(9) He, Z.; Liu, J.; Qiao, Y.; Li, C. M.; Tan, T. T. Y. Architecture Engineering of Hierarchically Porous Chitosan/Vacuum-Stripped Graphene Scaffold As Bioanode for High Performance Microbial Fuel Cell. *Nano Lett.* **2012**, *12*, 4738−4741.
(10) Janicek, A.; Fan, Y.; Liu, H. Design of Microbial Fuel Cells for Practical Application: A Review and Analysis of Scale-up Studies. *Biofuels* **2014**, *5*, 79−92.
(11) Tao, H.-C.; Sun, X.-N.; Xiong, Y. A Novel Hybrid Anion Exchange Membrane for High Performance Microbial Fuel Cells. *RSC Adv.* **2015**, *5*, 4659−4663.
(12) Nandy, A.; Kumar, V.; Mondal, S.; Dutta, K.; Salah, M.; Kundu, P. P. Performance Evaluation of Microbial Fuel Cells: Effect of Varying Electrode Configuration and Presence of a Membrane Electrode Assembly. *New Biotechnol.* **2014**, *32*, 272−281.
(13) Tao, Q.; Zhou, S. Effect of Static Magnetic Field on Electricity Production and Wastewater Treatment in Microbial Fuel Cells. *Appl. Microbiol. Biotechnol.* **2014**, *98*, 9879−9887.

DOI: 10.1021/acsami.5b03990
ACS Appl. Mater. Interfaces 2015, 7, 14501−14505

(14) Lin, C.-W.; Wu, C.-H.; Chiu, Y.-H.; Tsai, S.-L. Effects of Different Mediators on Electricity Generation and Microbial Structure of a Toluene Powered Microbial Fuel Cell. *Fuel* **2014**, *125*, 30−35.
(15) Zhang, B.; Wen, Z.; Ci, S.; Mao, S.; Chen, J.; He, Z. Synthesizing Nitrogen-Doped Activated Carbon and Probing its Active Sites for Oxygen Reduction Reaction in Microbial Fuel Cells. *ACS Appl. Mater. Interfaces* **2014**, *6*, 7464−7470.
(16) Zhao, C. e.; Wu, J.; Ding, Y.; Wang, V. B.; Zhang, Y.; Kjelleberg, S.; Loo, J. S. C.; Cao, B.; Zhang, Q. Hybrid Conducting Biofilm with Built-in Bacteria for High-Performance Microbial Fuel Cells. *ChemElectroChem* **2015**, *2*, 654−658.
(17) Yong, Y.-C.; Yu, Y.-Y.; Zhang, X.; Song, H. Highly Active Bidirectional Electron Transfer by a Self-Assembled Electroactive Reduced Graphene Oxide Hybridized Biofilm. *Angew. Chem., Inter. Ed.* **2014**, *53*, 4480−4483.
(18) Yuan, H.; He, Z. Graphene-Modified Electrodes for Enhancing the Performance of Microbial Fuel Cells. *Nanoscale* **2015**, *7*, 7022−7029.
(19) Wen, Z.; Ci, S.; Mao, S.; Cui, S.; Lu, G.; Yu, K.; Luo, S.; He, Z.; Chen, J. TiO_2 Nanoparticles-Decorated Carbon Nanotubes for Significantly Improved Bioelectricity Generation in Microbial Fuel Cells. *J. Power Sources* **2013**, *234*, 100−106.
(20) Zhao, C.; Gai, P.; Liu, C.; Wang, X.; Xu, H.; Zhang, J.; Zhu, J.-J. Polyaniline Networks Grown on Graphene Nanoribbons-Coated Carbon Paper with a Synergistic Effect for High-Performance Microbial Fuel Cells. *J. Mater. Chem. A* **2013**, *1*, 12587−12594.
(21) Qiao, Y.; Bao, S.-J.; Li, C. M.; Cui, X.-Q.; Lu, Z.-S.; Guo, J. Nanostructured Polyaniline/Titanium Dioxide Composite Anode for Microbial Fuel Cells. *ACS Nano* **2007**, *2*, 113−119.
(22) Jiang, X.; Hu, J.; Lieber, A. M.; Jackan, C. S.; Biffinger, J. C.; Fitzgerald, L. A.; Ringeisen, B. R.; Lieber, C. M. Nanoparticle Facilitated Extracellular Electron Transfer in Microbial Fuel Cells. *Nano Lett.* **2014**, *14*, 6737−6742.
(23) Garner, L. E.; Thomas, A. W.; Sumner, J. J.; Harvey, S. P.; Bazan, G. C. Conjugated Oligoelectrolytes Increase Current Response and Organic Contaminant Removal in Wastewater Microbial Fuel Cells. *Energy Environ. Sci.* **2012**, *5*, 9449−9452.
(24) Thomas, A. W.; Henson, Z. B.; Du, J.; Vandenberg, C. A.; Bazan, G. C. Synthesis, Characterization, and Biological Affinity of a Near-Infrared-Emitting Conjugated Oligoelectrolyte. *J. Am. Chem. Soc.* **2014**, *136*, 3736−3739.
(25) Wang, V. B.; Du, J.; Chen, X.; Thomas, A. W.; Kirchhofer, N. D.; Garner, L. E.; Maw, M. T.; Poh, W. H.; Hinks, J.; Wuertz, S.; Kjelleberg, S.; Zhang, Q.; Loo, J. S. C.; Bazan, G. C. Improving Charge Collection in *Escherichia coli*−Carbon Electrode Devices with Conjugated Oligoelectrolytes. *Phys. Chem. Chem. Phys.* **2013**, *15*, 5867−5872.
(26) Alves, F.; Nischang, I. Tailor-Made Hybrid Organic−Inorganic Porous Materials Based on Polyhedral Oligomeric Silsesquioxanes (POSS) by the Step-Growth Mechanism of Thiol-Ene "Click" Chemistry. *Chem.-A Eur. J.* **2013**, *19*, 17310−17313.
(27) Ferrer-Ugalde, A.; Juárez-Pérez, E. J.; Teixidor, F.; Viñas, C.; Núñez, R. Synthesis, Characterization, and Thermal Behavior of Carboranyl−Styrene Decorated Octasilsesquioxanes: Influence of the Carborane Clusters on Photoluminescence. *Chem.-A Eur. J.* **2013**, *19*, 17021−17030.
(28) Pu, K. Y.; Li, K.; Zhang, X.; Liu, B. Conjugated Oligoelectrolyte Harnessed Polyhedral Oligomeric Silsesquioxane as Light-Up Hybrid Nanodot for Two-Photon Fluorescence Imaging of Cellular Nucleus. *Adv. Mater.* **2010**, *22*, 4186−4189.
(29) Garner, L. E.; Park, J.; Dyar, S. M.; Chworos, A.; Sumner, J. J.; Bazan, G. C. Modification of the Optoelectronic Properties of Membranes via Insertion of Amphiphilic Phenylenevinylene Oligoelectrolytes. *J. Am. Chem. Soc.* **2010**, *132*, 10042−10052.
(30) Woo, H. Y.; Liu, B.; Kohler, B.; Korystov, D.; Mikhailovsky, A.; Bazan, G. C. Solvent Effects on the Two-Photon Absorption of Distyrylbenzene Chromophores. *J. Am. Chem. Soc.* **2005**, *127*, 14721−14729.
(31) Pu, K.-Y.; Liu, B. Fluorescence Turn-on Responses of Anionic and Cationic Conjugated Polymers toward Proteins: Effect of Electrostatic and Hydrophobic Interactions. *J. Phys. Chem. B* **2010**, *114*, 3077−3084.
(32) Hou, H.; Chen, X.; Thomas, A. W.; Catania, C.; Kirchhofer, N. D.; Garner, L. E.; Han, A.; Bazan, G. C. Conjugated Oligoelectrolytes Increase Power Generation in *E. coli* Microbial Fuel Cells. *Adv. Mater.* **2013**, *25*, 1593−1597.
(33) Wang, V. B.; Yantara, N.; Koh, T. M.; Kjelleberg, S.; Zhang, Q.; Bazan, G. C.; Loo, S. C. J.; Mathews, N. Uncovering Alternate Charge Transfer Mechanisms in *Escherichia coli* Chemically Functionalized with Conjugated Oligoelectrolytes. *Chem. Commun.* **2014**, *50*, 8223−8226.

DOI: 10.1021/acsami.5b03990
ACS Appl. Mater. Interfaces 2015, 7, 14501−14505